ELECTRONIC SUPPLEMENTARY INFORMATION (ESI)

Rationally designed rare earth separation by selective oxalate solubilization

Denis Prodius,[a] Matthew Klocke,[b] Volodymyr Smetana,[a, c] Tarek Alammar,[b] Marilu Perez Garcia,[a] Theresa L. Windus,[a, d] Ikenna C. Nlebedim,[a] Anja-Verena Mudring*[a, b, c]

[a]Ames Laboratory, US Department of Energy and Critical Materials Institute, Ames, Iowa 50011-3020, USA

[b]Department of Materials Sciences and Engineering, Iowa State University, Ames, Iowa 50011-1096, USA

[c]Department of Materials and Environmental Chemistry, Stockholm University, Svante Arrhenius väg 16C, 106 91 Stockholm, Sweden. E-mail: anja-verena.mudring@mmk.su.se

[d]Department of Chemistry, Iowa State University, Ames, Iowa 50011-3111, USA

Table of contents

1.	Synthesis	ESI p. 2-5
2.	X-ray analysis	ESI p. 6-9
3.	Raman spectra	ESI p. 12-13
4.	Computations	ESI p, 14-20
5.	Thermal Characterization	ESI p. 21

1. Synthesis

(a) In a typical one stage bench-scale testing, to an aqueous solution of oxalic acid ($H_2C_2O_4 \cdot 2H_2O$, 10 mmol, 1.2607 g) and the organic base (20 mmol) in 10 mL of water, the specific quantity (up to ~1.6 mmol; standard deviation for the amount of dissolved individual RE oxalate is about 7%) of $RE_2(ox)_3 \cdot nH_2O$ (where RE = Y for **3**, n = 10 (for La-Er[#]) [**R1**] and 6 (for Er[##]-Lu) [**R2**]) was added under stirring. The mixture was stirred for 15 min at 100°C (Eq. S1). To identify the structural units in these soluble oxalate complexes, the single crystal x-ray diffraction (SXRD) technique has been applied. The resulting solutions were allowed to stand undisturbed for slow evaporation and single crystals growth. As an example, after about one week suitable for SXRD colourless crystals (**3**) were collected by filtration, washed quickly with cold water and dried in air. (b) Dissolution in ethanolic solution: similar to procedure (a) except of water (10 mL) was replaced with 10 mL of ethanol (96%); (c) The rare-earth(III) oxalates derived from the recycling of NdFeB magnets (from motors) and identified as $RE_2(C_2O_4)_3 \cdot 10H_2O$ (RE = Nd, Pr, Dy; 102 mg) have been applied for the following separation similarly as described above for the procedure (a). An equivalent amount of diluted H_3PO_4 (~10%) was added to the extracted solution to precipitate a rare earth-containing insoluble phase ($REPO_4$).

$$x RE_2(C_2O_4)_3 \cdot nH_2O + H_2C_2O_4 \cdot 2H_2O + 2Base \rightarrow [H_3O]_m(Base\text{-}H^+)_a[RE(C_2O_4)_b](H_2O)_c \quad \text{(Eq. S1)}$$

where x = 0.01÷1.6; n = 10 (RE = La to Er) and 6 (RE = Er to Lu); m = 0 or 1; a = 1, 3, 4, 5, 8; b = 2, 3, 4, 7; c = 1,1.5, 2 and 10; Base = 1-methylimidazole, 1-ethylimidazole, N-methylpyrrolidine.

Yield (based on Y): ~342 mg (~66 %). Anal. calc. for $C_{28}H_{39}N_{10}O_{18}Y$ (**3**): C, 37.67; H, 4.41; N, 15.69; Found: C, 37.72; H, 4.30; N, 15.71. IR, cm^{-1}: 3384 (wm, br), 3104 (w), 3026 (w), 2953 (vw), 2819 (vw), 2713 (vw, br), 2603 (vw, br), 1611 (vs), 1549 (w), 1421 (s, sh), 1376 (w), 1284 (s), 1188 (w), 1160 (w), 1083 (mw, br), 994 (mw, br), 886 (m), 839 (w), 777 (s), 666 (w), 619 (m), 483 (ms).

- - - -

≡ synthesized at RT; ## ≡ synthesized at 100°C.

[**R1**] For lanthanide ions ranging from La to Er[#], the chemical formula is $Ln_2(C_2O_4)_3(H_2O)_6 \cdot 4H_2O$:
(a) E. Hansson, *Acta Chem. Scand.* **24** (1970) 2969; (b) E. Hansson, *Acta Chem. Scand.* **27** (1973) 823.

[**R2**] For lanthanide ions ranging from Er[##] to Lu, the chemical formula is $Ln_2(C_2O_4)_3(H_2O)_4 \cdot 2H_2O$:
E. Hansson, *Acta Chem. Scand.* **26** (1970) 1337.

The chemicals (1-methylimidazole, 1-ethylimidazole, N-methylpyrrolidine, oxalic acid) were of ACS reagent grade (>99%, *Sigma-Aldrich*) and used as received. Compounds **L1**, **L2·H$_2$O** and **3** (Y) were analyzed by CHN elemental analysis (Elementar Vario EL Analyzer, Hanau, Germany) and infrared spectroscopy (Agilent Cary 630 FTIR Spectrometer, Santa Clara, California, USA). Attenuated total reflectance (ATR) spectroscopy was carried out on an Agilent Technologies Cary 630 FT-IR spectrometer equipped with a diamond-crystal ATR unit. Solid samples were pressed on top of the ATR crystal with a diamond surface to ensure contact. Raman spectra were obtained at 150 mW on a Horiba Xplora Raman microscope at RT.

$[(mimH)_3(HC_2O_4)(C_2O_4)]$ (L1) and $[(mimH)(HC_2O_4)]$ H_2O (L2·H_2O):

The ligands **L1** and **L2·H_2O** have been obtained by mixing 1-methylimidazole and oxalic acid (10 mmol) in hot water (10 mL, t ≈60-65°C) according to the Scheme S1:

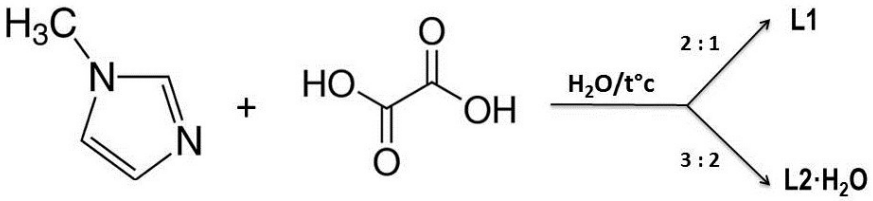

Scheme S1. Synthesis of **L1** and **L2·**H_2O ligands.

After cooling to the room temperature, the resulting aqueous solutions were allowed to stand undisturbed for slow evaporation on air and single crystals growth (between 1 to 2 weeks).

Yield (based on oxalic acid): ~48% (2.05 g). Anal. calc. for $C_{16}H_{22}N_6O_8$ (**L1**): C, 45.06; H, 5.21; N, 19.71; Found: C, 44.92; H, 5.14; N, 19.86. IR, cm^{-1}: 3104 (w), 3041 (w, br), 1702 (w), 1601 (s), 1570 (s), 1547 (s), 1452 (mw), 1406 (mw), 1275 (s, sh), 1167 (w), 1111 (w, sh), 1079 (w, sh), 867 (m), 844 (m), 746 (m, sh), 723 (m, br), 660 (w, sh), 621 (vs, sh), 488 (m), 442 (m).

Yield (based on oxalic acid): ~76% (1.45 g). Anal. calc. for $C_6H_{10}N_2O_5$ (**L2·H_2O**): C, 37.89; H, 5.31; N, 14.73; Found: C, 37.77; H, 5.20; N, 14.66. IR, cm^{-1}: 3104 (w), 3040 (w, br), 1702 (w, br), 1601 (s), 1570 (s), 1547 (s), 1452 (w), 1406 (w), 1275 (s, sh), 1169 (w), 1111 (w, sh), 1079 (w, sh), 867 (ms), 746 (m, sh), 723 (m, br), 621 (s, sh), 488 (m, br), 442 (m).

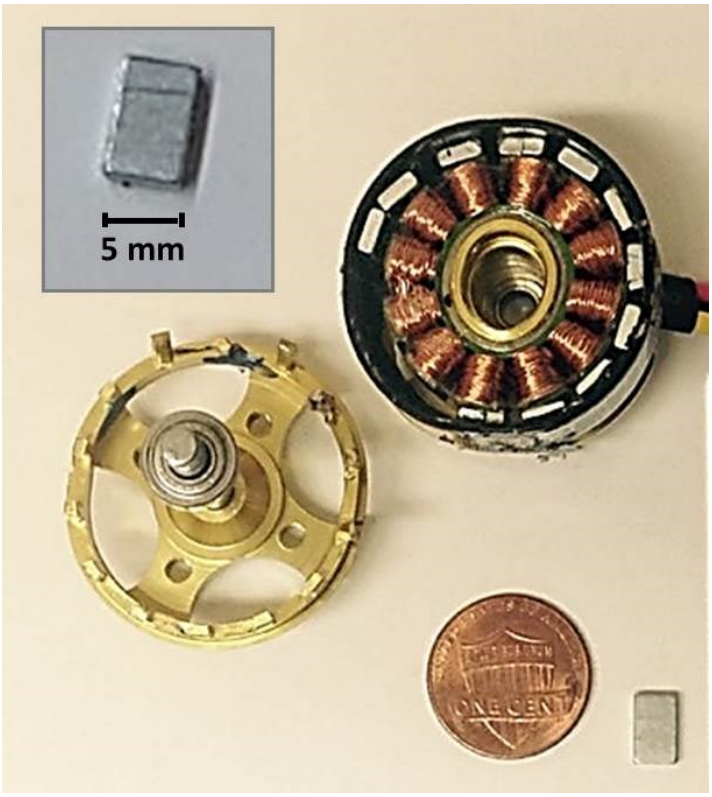

Figure S1. Dismantled "Great Planes RimFire .10 35-30-1250 Outrunner Brushless" motor with inset showing RE magnet removed from the motor.

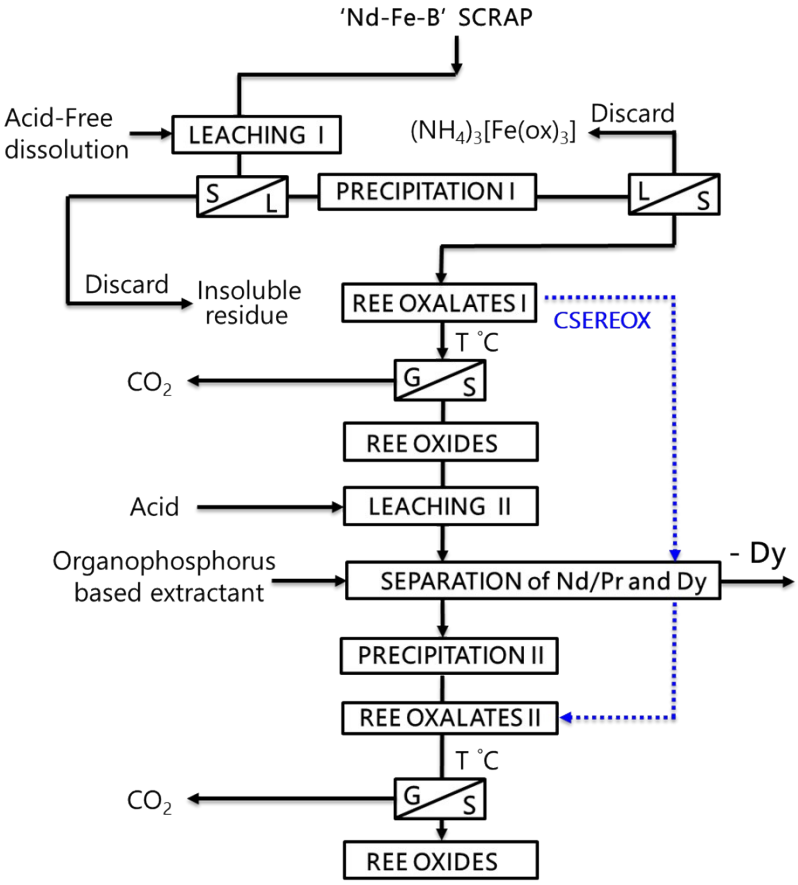

Figure S2. A general overview of the REE recovery process for neodymium-iron-boron (Nd-Fe-B) magnet scrap processed by acid-free dissolution approach [ref.12, in manuscript] and traditional solvent extraction route, in comparison to the newly developed CSEREOX procedure (dotted blue line). ox ≡ oxalate anion ($C_2O_4^{2-}$). [ref. 12]: D. Prodius, K. Gandha, A.-V. Mudring and I. C. Nlebedim, *ACS Sustain. Chem. Eng.*, 2020, **8** (3), 1455–1463.

2. Single X-ray structure analysis

The X-ray measurements were performed at 100(2)K on a Bruker D8 Venture diffractometer operating at 50 kV and 1 mA equipped with Photon 100 CMOS detector a flat graphite monochromator and a Mo K_α IμS micro-focus source (λ = 0.71073 Å). The raw frame data were collected using the Bruker APEX3 program [S1], while the frames were integrated with the Bruker SAINT software package [S2] using a narrow-frame algorithm integration of the data and were corrected for absorption effects using the multi-scan method (SADABS) [S3]. The non-hydrogen atoms were refined anisotropically. All hydrogen atoms were placed in their calculated positions and refined within the relying model. Initial models of the crystal structures were first obtained with the program SHELXT-2014 [S4] and refined using the program SHELXL-2014 [S5] within the APEX3 software package.

[S1] APEX3, Bruker AXS Inc., Madison, Wisconsin, USA, 2015.
[S2] SAINT, Bruker AXS Inc., Madison, Wisconsin, USA, 2015.
[S3] Krause, L.; Herbst-Irmer, R.; Sheldrick, G. M.; Stalke, D. *J. Appl. Crystallogr.* **2015**, *48*, 3.
[S4] Sheldrick, G. M. *Acta Crystallogr. A* **2015**, *71*, 3.
[S5] Sheldrick, G. M. *Acta Crystallogr. C* **2015**, *71*, 3.

Table S1. Crystallographic data, details of data collection and structure refinement parameters for **L1**, **L2**·H_2O**, 1**-**12**.

	L1	**L2**·H_2O	**1**	**2**	**3**
Empirical formula	$C_{16}H_{22}N_6O_8$	$C_{12}H_{20}N_4O_{10}$	$C_{16}H_{14}Ho_2N_4O_{20}$	$C_8H_7ErN_2O_{10.5}$	$C_{28}H_{39}N_{10}O_{18}Y$
Formula weight	426.40	380.31	912.17	466.42	888.57
Temperature/K	296	173	296	296	173
Crystal system	triclinic	monoclinic	monoclinic	monoclinic	monoclinic
Space group	P-1	$P2_1/c$	$P2_1/n$	$C2$	Cc
a/Å	7.6321(11)	11.8129 (2)	10.023(2)	14.6700(13)	12.0684(3)
b/Å	10.9503(16)	10.3804(2)	17.357(4)	11.5086(10)	17.5403(4)
c/Å	12.4367(18)	6.9487 (1)	14.354(3)	9.1980(10)	18.0493(4)
α/deg	92.390(3)	90	90	90	90
β/deg	95.911(2)	100.2700 (13)	99.312(12)	121.4040(10)	98.6850(10)
γ/deg	100.137(3)	90	90	90	90
V/Å^3	1015.8(3)	838.42 (3)	2464.1(9)	1325.4(2)	3776.93(15)
Z	4	2	4	4	4
F000	448	400	1728	900	1824
ρ_{calc}/g/cm^3	1.859	1.5063	2.459	2.337	1.563
μ/mm^{-1}	0.113	0.132	6.48	6.396	1.634
ϑ_{min}, ϑ_{max}(°)	1.89 to 26.31	2.63 to 26.99	4.015 to 30.888	4.11 to 31.10	2.06 to 31.90
Reflections collected	16650	21310	32483	7723	50715
Independent reflections	4109 [R_{int} = 0.0792]	2331[R_{int} = 0.0399]	7498 [R_{int} = 0.1564]	3961 [R_{int} = 0.0184]	12931 [R_{int} = 0.0761]
Data/restraints/parameters	4109/0/254	2331/0/133	7498 /0/379	3961/1/188	12931/2/514
Flack parameter				0.48(1)	0.25(7)
GOF[c]	0.976	1.0609	0.957	0.867	0.949
R_1[a](I>2σ(I))	0.0549	0.0542	0.0517	0.0280	0.0556

wR_2[b](all data)	0.1839	0.1632	0.1504	0.1018	0.1592
Largest diff. peak/hole/e Å^{-3}	0.27/-0.20	0.61/-0.54	3.22/-3.53	1.80/-1.01	0.73/-0.49
CCDC number	1554317	1554318	1554327	1554325	1554329

[a] $R_1 = \Sigma||F_o| - |F_c||/\Sigma|F_o|$, [b] $wR_2 = \{\Sigma[w\,(F_o^2 - F_c^2)^2]\,/\Sigma[w(F_o^2)^2]\}^{1/2}$. [c] GOF = $\{\Sigma[w(F_o^2 - F_c^2)^2]\,/(n-p)\}^{1/2}$, where n is the number of reflections and p is the total number of parameters refined

continued (part 2)

	4	**5**	**6**	**7**	**8**	**9**
Empirical formula	$C_{28}H_{35}N_{10}O_{18}Yb$	$C_{28}H_{35}LuN_{10}O_{18}$	$C_9H_9HoN_2O_{10}$	$C_{21}H_{27}N_6O_{14}Yb$	$C_{27}H_{48}N_4O_{19}Tm$	$C_{27}H_{48}N_4O_{19}Yb$
Formula weight	972.67	974.63	470.11	760.52	901.62	905.73
Temperature/K	296	296	296	296	293	173
Crystal system	monoclinic	monoclinic	monoclinic	triclinic	triclinic	triclinic
Space group	*Cc*	*Cc*	$P2_1/n$	P-1	P-1	P-1
a/Å	12.034(2)	12.0002(2)	9.6712(2)	8.8524(18)	11.897(7)	11.61220(10)
b/Å	17.556(4)	17.5085(3)	11.3857(3)	10.434(2)	12.988(8)	12.8415(2)
c/Å	18.359(4)	18.0660(4)	12.6870(3)	15.937(3)	14.598(11)	14.4646(2)
α/deg	90	90	90	87.131(2)	63.692(6)	64.1820(10)
ß/deg	98.44(3)	98.6189 (8)	96.4750(10)	87.135(2)	79.555(10)	80.6390(10)
γ/deg	90	90	90	88.571(2)	74.701(7)	75.3080(10)
V/Å^3	3836.6	3752.90(12)	1388.10(6)	1468.0(5)	1945(2)	1874.77(5)
Z	4	4	4	2	2	2
*F*000	1948	1952	896	754	918	920
ρ_{calc}/g/cm^3	1.722	1.725	2.250	1.721	1.540	1.604
μ/mm^{-1}	2.582	2.721	5.756	3.260	2.359	2.575
ϑ_{min}, ϑ_{max}(°)		2.073 to 42.136	2.410 to 36.693	2.284 to 26.624	1.78 to 32.45	1.567 to 46.828
Reflections collected		61720	27996	23529	44446	72004

Independent reflections	23248 [R_{int} = 0.0421]	6566 [R_{int} = 0.0564]	6085 [R_{int} = 0.0487]	10502 [R_{int} = 0.0355]	28918 [R_{int} = 0.0267]
Data/restraints/parameters	23248/0/254	6566/0/187	6085/1/373	10502/0/208	28918/2/410
Flack parameter	0.171(9)				
GOF[c]	0.739	0.999	0.907	0.936	0.748
R_1[a]($I>2\sigma(I)$)	0.0367	0.0411	0.0457	0.0394	0.0489
wR_2[b](all data)	0.1099	0.1051	0.1205	0.1300	0.2008
Largest diff. peak/hole/e Å^{-3}	2.16/-1.37	2.69/-2.20	3.47/-2.09	1.29/-0.79	2.76/-2.65
CCDC number	1554328	1554323	1554320	1554322	1554324

[a] $R_1 = \Sigma||F_o| - |F_c||/\Sigma|F_o|$, [b] $wR_2 = \{\Sigma[w\,(F_o^2 - F_c^2)^2]\,/\Sigma[w(F_o^2)^2]\}^{1/2}$. [c] GOF = $\{\Sigma[w(F_o^2 - F_c^2)^2]\,/(n-p)\}^{1/2}$, where n is the number of reflections and p is the total number of parameters refined

continued (part 3)

	10	**11**	**12**
Empirical formula	$C_{24}H_{28}HoN_8O_{18}$	$C_{24}H_{28}N_8O_{18}Tm$	$C_{24}H_{28}LuN_8O_{18}$
Formula weight	881.47	885.47	891.51
Temperature/K	296	296	296
Crystal system	monoclinic	monoclinic	monoclinic
Space group	*Cc*	*Cc*	*Cc*
a/Å	12.0981(19)	12.0526(19)	12.038(5)
b/Å	17.5518(19)	17.5649(19)	17.562(5)
c/Å	18.316(2)	18.317(2)	18.345(7)
α/deg	90	90	90
ß/deg	98.538(7)	98.558(7)	98.384(5)
γ/deg	90	90	90
V/Å^3	3846.1(9)	3834.6(9)	3837(2)
Z	4	4	4

$F000$	1756	1764	1772
ρ_{calc}/g/cm^3	1.522	1.534	1.543
μ/mm^{-1}	2.136	2.392	2.652
ϑ_{min}, ϑ_{max}(°)	2.06 to 36.44	2.06 to 43.57	4.41 to 32.02
Reflections collected	81138	87872	62090
Independent reflections	17907 [R_{int} = 0.0532]	27782 [R_{int} = 0.0442]	12745 [R_{int} = 0.0315]
Data/restraints/parameters	17907/2/271	27782/2/271	12745/6/460
Flack parameter	0.44(2)	0.37(2)	0.47(2)
GOF[c]	1.083	0.966	1.071
R_1[a](I>2σ(I))	0.0580	0.0558	0.0415
wR_2[b](all data)	0.1747	0.1739	0.1255
Largest diff. peak/hole/e Å^{-3}	2.96/-1.41	3.00/-1.64	2.28/-0.60
CCDC number	1554319	1554326	1554321

[a] $R_1 = \Sigma||F_o| - |F_c||/\Sigma|F_o|$, [b] $wR_2 = \{\Sigma[w\,(F_o^2 - F_c^2)^2]\,/\Sigma[w(F_o^2)^2]\}^{1/2}$. [c] GOF = $\{\Sigma[w(F_o^2 - F_c^2)^2]\,/(n-p)\}^{1/2}$, where n is the number of reflections and p is the total number of parameters refined.

The crystal quality of **4** did not allow for a complete structure refinement.

SXRD has also been used to gain an understanding of the interaction of oxalic acid with the base in absence of RE(III). We have evidenced two different stages of proton transfer from oxalic acid to the base, *i.e.* $[(mimH)_3(HC_2O_4)(C_2O_4)]$ (**L1**) and $[(mimH)(HC_2O_4)]\cdot H_2O$ (**L2**). In **L1**, the oxalate anions form dimers connected through a proton, while the charge is compensated by three 1-methylimidazolium cations interacting with the anions through the N–H–O hydrogen bonds (SI, Fig. S1). The imidazole inter-ring separations within neighboring associates range from 3.7 to 4.1 Å, indicating possible π-π interaction between the latter. A considerably different situation is observed for **L2**. Here, the monoprotonated oxalate anions form a polymeric chain featuring head-to-tail hydrogen bonds. Oxygen atoms that are involved in hydrogen bonding to another hydrogenoxalate anion are also hydrogen bonded to the protons of the imidazolium cations, whilst the remaining oxygen atoms of the anions are undergoing hydrogen bond interactions to the solvent water. Along with this N–H–O and O–H–O hydrogen bond network, supramolecular π-π interactions between the imidazole rings separated by 3.6 Å, are observed in this structure.

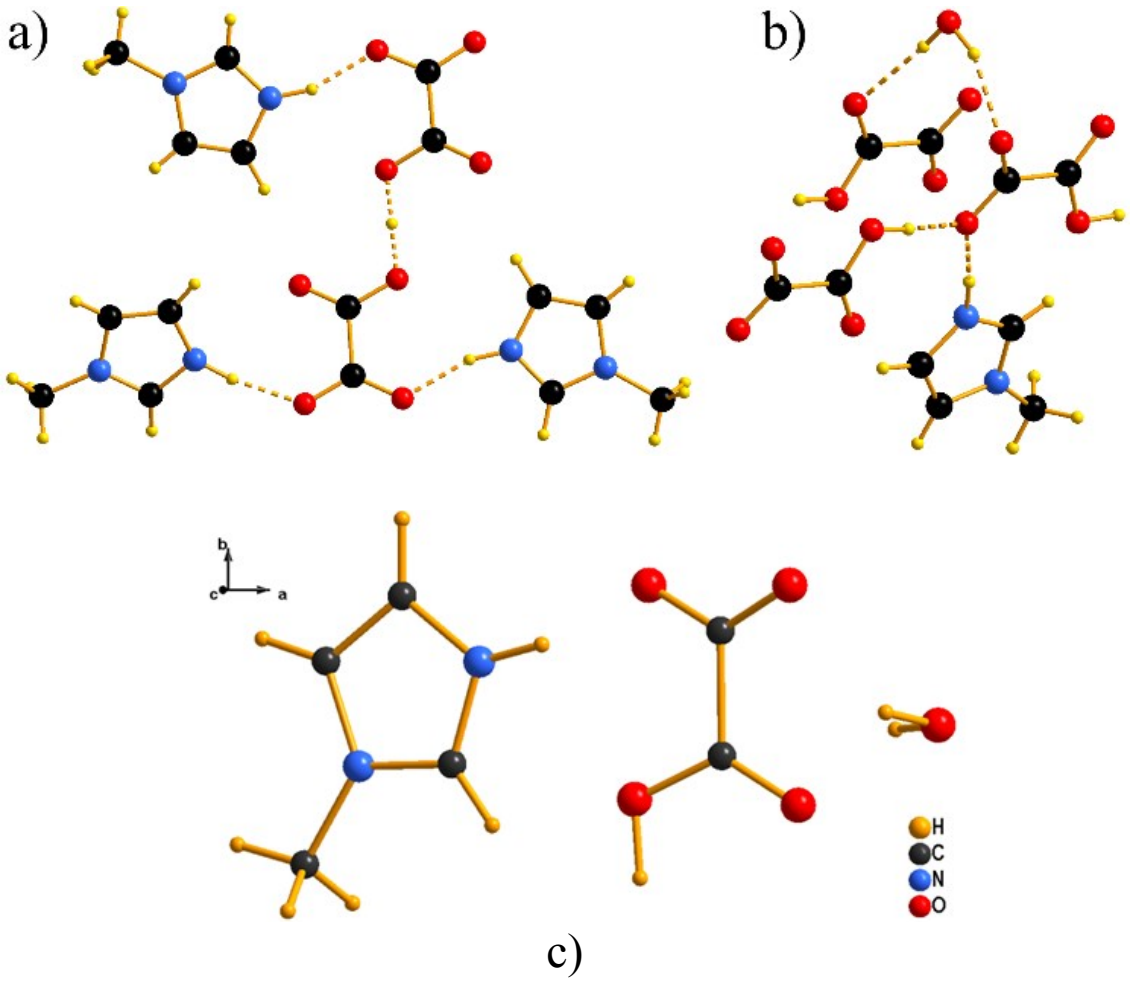

Figure S3. Molecular structures of $[(mimH)_3(HC_2O_4)(C_2O_4)]$ (**L1**) (a) and $[(mimH)(HC_2O_4)]\cdot H_2O$ (**L2**) (b, c) fragments. Atom design: Carbon (black), oxygen (red), nitrogen (blue), hydrogen (yellow).

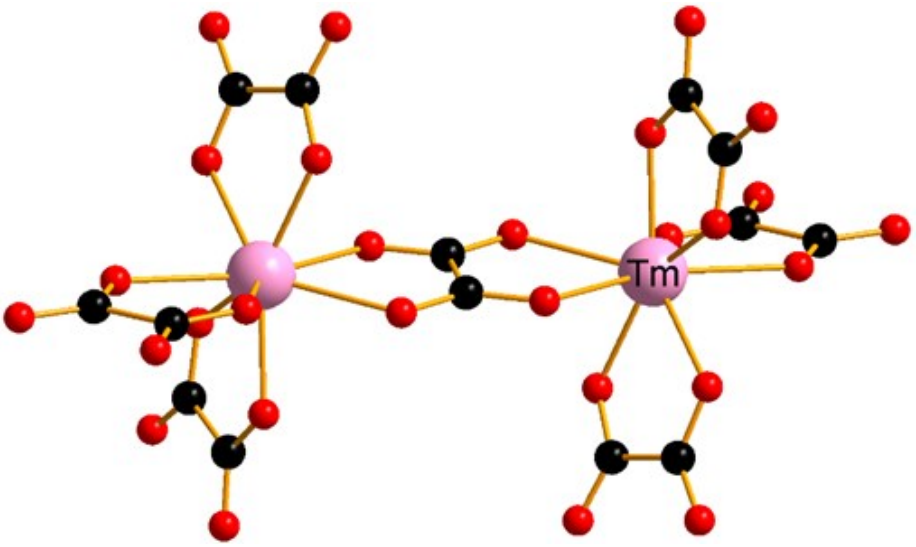

Figure S4. Structure of the $[Tm_2(C_2O_4)_7]^{8-}$ fragment in **8**. Counter-cations and water molecules were omitted for clarity. Atom design: Carbon (black), oxygen (red).

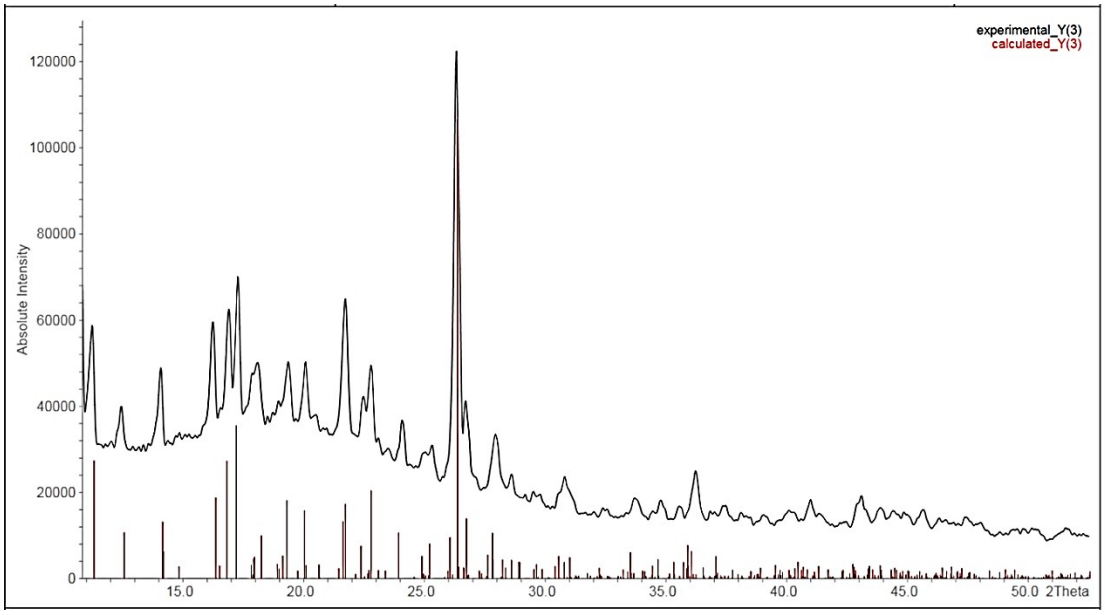

Figure S5. Comparison of calculated and measured X-ray powder diffraction patterns for **3**.

3. Raman Spectra

Raman spectra were obtained at 150 mW on a Horiba Xplora Raman microscope at room temperature. Laser irradiation of 785 nm was used for excitation. Silicon was used as a standard for the calibration of Raman shifts.

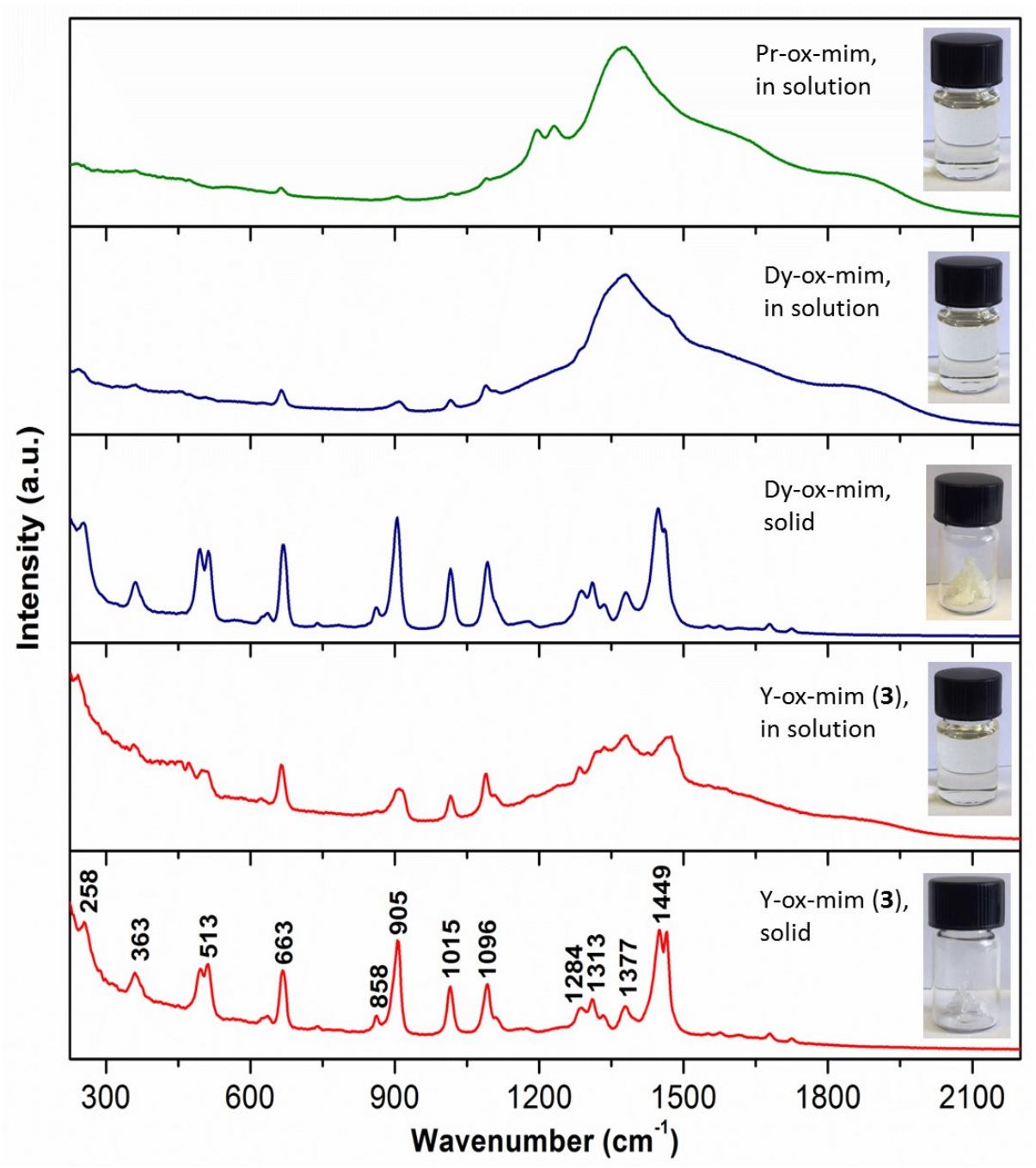

Figure S6. Raman spectra of RE containing oxalates in solid form and in aqueous solutions. RE-ox-mim ≡ rare earth oxalate with 1-methylimidazolium.

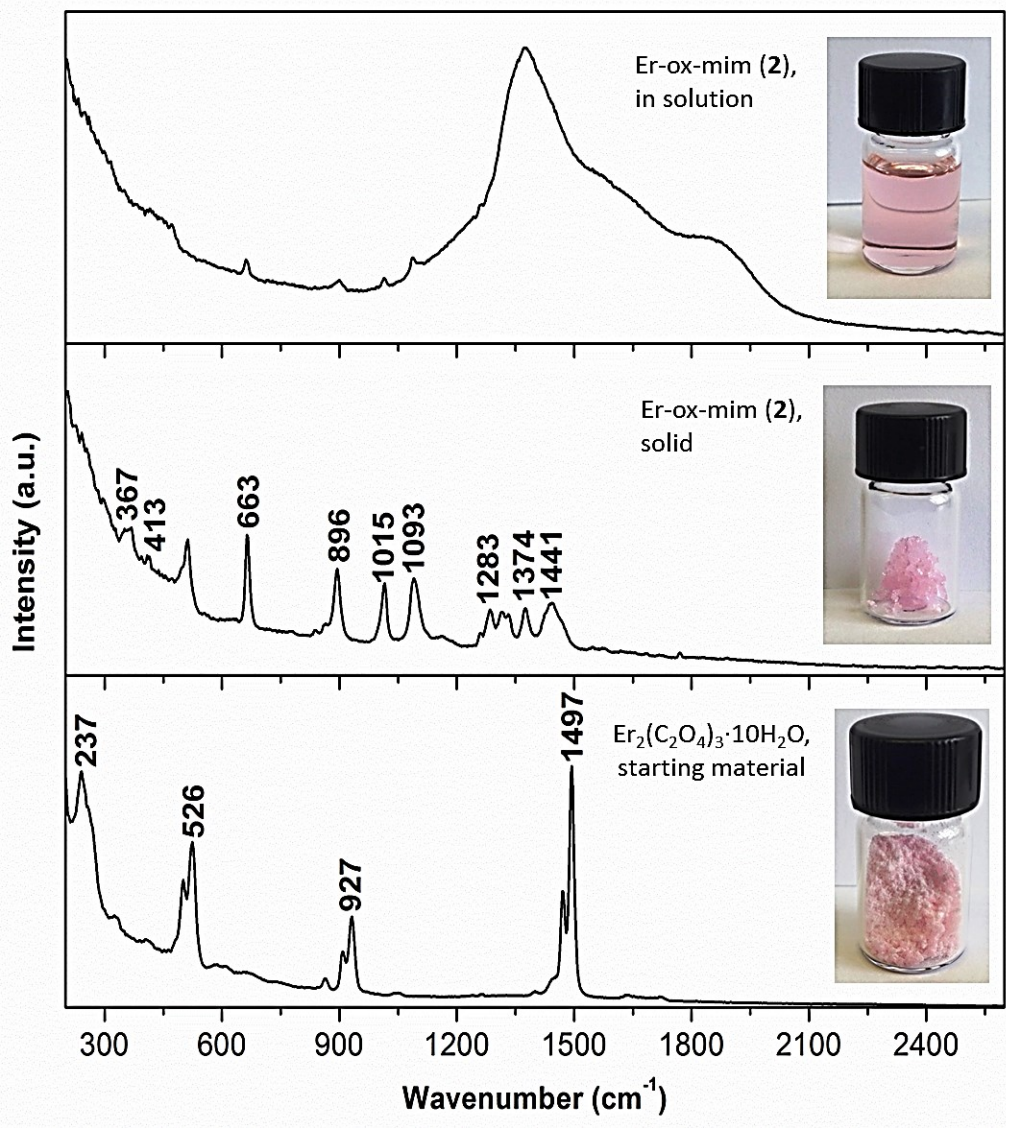

Figure S7. Raman spectra of erbium containing oxalates in solid (starting oxalate $Er_2(C_2O_4)_3 \cdot 10H_2O$ and **2**) and in aqueous solution (**2**). Er-ox-mim ≡ erbium oxalate with 1-methylimidazolium.

As shown in Figs. S6 and S7, the bands near 520 cm^{-1} can be assigned to the oxalate deformations δ_3(OCO) and δ_6(OCO). The bands around 943 cm^{-1} are attributed to the C-C stretching mode. Bands observed at 1497 cm^{-1} are assigned to the stretching of C-O band. The bands at 246 cm^{-1} and 363 cm^{-1} may be attributed to the Er-O stretching and bending modes respectively [S7].

[S7] (a) C. Tamain, B. Arab-Chapelet, M. Rivenet, X. F. Lego, G. Loubert, S. Grandjean, F. Abraham, *Inorg. Chem.* **2016**, *55*, 51−61; (b) R. L. Frost, A. Locke, W. N. Marten, *J. Raman Spectrosc.* **2008**, *39*, 901-908.

4. Computations

4.1 Methods

The relative binding energy between lanthanides was determined by comparing the ion exchange reaction described by the equation:

$$\left[Gd(NO_3)_3(H_2O)_2\right]_{(aq)} + \left[Ln(ox)(H_2O)_6\right]^+_{(aq)} \rightleftharpoons \left[Ln(NO_3)_3(H_2O)_2\right]_{(aq)} + \left[Gd(ox)(H_2O)_6\right]^+_{(aq)}$$

where Gd^{3+} is bound to a weakly coordinating ion, nitrate, and displaces Ln to form the $[Gd(ox)(H_2O)_6]^+$ hydrated product. The preferential binding, or relative binding energy is determined by whether the reaction is endo or exothermic. If the reaction is endothermic, the RE-oxalate has tighter binding than the Gd-ox, with the reverse being true for the exothermic reaction.

The minimum energy structures (SI Sect. 4.2) were calculated for each of the species in the equation with Ln=La and Lu. The geometries were equilibrated in gas phase and all but the $Gd(NO_3)_3(H_2O)_2$ were confirmed to be minima upon calculating positive definite Hessians. The solvent phase energies were corrected with zero-point energy and thermal corrections derived from gas phase calculations. Solvent phase single point energies were calculated for gas phase geometries using the SMD implicit solvent method [S8] and restricted open-shell DFT. All calculations were run using NWChem [S9] with B3LYP [S10] level of theory and 6-31+G* basis [S11] for non-lanthanide elements and Stuttgart effective core potential and basis [S12] for the lanthanides.

[S8] (a) Mantina, M.; Valero, R.; Cramer, C. J.; Truhlar, D. G., Atomic Radii of the Elements. In *CRC Handbook of Chemistry and Physics*, 91 ed.; Haynes, W. M., Ed. CRC Press: Boca Raton, FL, 2010; pp 49-50. (b) Marenich, A. V.; Cramer, C. J.; Truhlar, D. G., Universal Solvation Model Based on Solute Electron Density and on a Continuum Model of the Solvent Defined by the Bulk Dielectric Constant and Atomic Surface Tensions. *The Journal of Physical Chemistry B* **2009,** *113* (18), 6378-6396. (c) Winget, P.; Dolney, D. M.; Giesen, D. J.; Cramer, C. J.; Truhlar, D. G., *Minnesota Solvent Descriptor Database*. University of Minnesota: Minneapolis, MN, 2010.

[S9] M. Valiev, E.J. Bylaska, N. Govind, K. Kowalski, T.P. Straatsma, H.J.J. van Dam, D. Wang, J. Nieplocha, E. Apra, T.L. Windus, W.A. de Jong, *Comput. Phys. Commun.* **2010**, *181*, 1477.

[S10] (a) Becke, A. D. *J. Chem. Phys.* **1993**, 98 (7), 5648. (b) Lee, C.; Yang, W.; Parr, R. G. *Phys. Rev. B: Condens. Matter Mater. Phys.* **1988**, 37 (2), 785−789.

[S11] (a) 1. Clark, T.; Chandrasekhar, J.; Spitznagel, G. W.; Schleyer, P. V. R., *Journal of Computational Chemistry* **1983***, 4* (3), 294-301. (b) Francl, M. M.; Pietro, W. J.; Hehre, W. J.; Binkley, J. S.; Gordon, M. S.; DeFrees, D. J.; Pople, J. A., *The Journal of Chemical Physics* **1982**, *77* (7), 3654-3665. (c) Gill, P. M. W.; Johnson, B. G.; Pople, J. A.; Frisch, M. J., *Chem. Phys. Let.* **1992**, *197* (4), 499-505. (d) Hariharan, P. C.; Pople, J. A., *Theoretica Chimica Acta* **1973**, *28*, 213. (c) Krishnan, R.; Binkley, J. S.; Seeger, R.; Pople, J. A., *The Journal of Chemical Physics* **1980***, 72* (1), 650-654.

[S12] (a) Cao, X.; Dolg, M., *Journal of Molecular Structure: THEOCHEM* **2002,** *581* (1–3), 139-147. (b) Dolg, M.; Stoll, H.; Preuss, H., *The Journal of Chemical Physics* **1989,** *90* (3), 1730-1734. (c) Cao, X.; Dolg, M., *The Journal of Chemical Physics* **2001,** *115* (16), 7348-7355.

Table S2. For each metal center (Ln^{3+}), the following distances in units of angstroms are provided: ionic radius [S13], average interatomic distance between metal ion and oxygen in the crystal structure, average simulated lanthanide to oxalate-oxygen interatomic distance, and simulated lanthanide to water-oxygen interatomic distance. The last column gives the coordination number observed in the crystal structures and used in simulations of Lu^{3+}, Gd^{3+}, and La^{3+}.

Ln^{3+}	ionic radius (Å)	Crystal Ln^{3+}-O (Å)	Sim. Ln^{3+}-O_{ox} (Å)	Sim M^{3+}-O_{water} (Å)	Coord. number
La^{3+}	1.160	-	2.28	2.68	8
Gd^{3+}	1.053	-	2.18	2.56	8
Dy^{3+}	1.027	2.37	-	-	8
Y^{3+}	1.019	2.35	-	-	8
Ho^{3+}	1.015 (1.072)	2.43	-	-	8 (9)
Er^{3+}	1.004 (1.062)	2.41	-	-	8 (9)
Lu^{3+}	0.977	2.31	2.13	2.44	8

Table S3. Sum of the reactant (E_{react}) and product (E_{prod}) energies, including thermal and zero-point energy corrections and the energy of the reaction, $\Delta E = E_{prod}-E_{react}$.

Ln^{3+}	E_{react} (hartrees)	E_{prod} (hartrees)	ΔE (hartrees)	ΔE (kcal/mol)
Lu^{3+}	-3831.512643	-3831.509449	0.003194	2.00
La^{3+}	-3030.861814	-3030.861785	0.000029	0.02

[S13] Huang, C.; Bian, Z., Introduction. In *Rare Earth Coordination Chemistry: Fundamentals and Applications*, Huang, C., Ed. John Wiley & Sons, Ltd: Chichester, UK, 2010; pp 1-39.

4.2 Minimum Energy Structures

The coordinates for all the structures used to calculate the values in Table S3 are found below. The geometries were optimized in gas phase as described in section 4.1 Methods.
E_{gas} and E_{water} are the energy in gas phase and aqueous phase in Hartrees, respectively. $E_{zpe/th}$ is the zero-point energy correction plus the thermal correction to 298.15 K.

1. $[La(ox)(H_2O)_6]^+$

E_{gas} = -1271.426775452002
E_{water} = -1271.590562891817
$E_{ZPE/Th}$ = 0.369996

La	-0.13513619	0.82655591	0.30037331
O	0.12682417	1.29253720	2.83813108
H	-0.35562397	1.02019104	3.63588240
H	1.08127048	1.27912221	3.04493284
O	0.11235456	3.42215316	-0.31325887
H	0.58635637	3.57441990	-1.15020325
H	-0.04235469	4.29330848	0.08843578
O	-1.69669994	0.95540147	-1.97133465
H	-1.94476095	0.00930951	-1.85524540
H	-2.46427897	1.42201240	-2.34095830
O	1.00625684	1.34137242	-2.04855197
H	0.28926737	1.16316398	-2.68924196
H	1.81086877	0.91975529	-2.39599110
O	-2.50711703	0.43850055	1.33813251
H	-2.72219003	-0.42703053	0.93226145
H	-3.27619871	0.73716865	1.85005447
O	-1.20114359	-1.09678150	-0.40789029
O	2.40288503	1.16180651	1.31626062
C	0.91984317	-2.19352497	-0.00022198
C	-0.57539106	-2.28350977	-0.47594619
O	-1.07359044	-3.31131218	-0.85959096
O	1.65537395	-3.14705961	0.01463490
O	1.25665478	-0.94706892	0.36591182
H	3.22340818	1.67774591	1.25795815
H	2.61479112	0.22078123	1.11343384

2. $[Gd(ox)(H_2O)_6]^+$

E_{gas} = -1601.5332202776
E_{water} = -1601.4839301272
$E_{ZPE/Th}$ = 0.370867

Gd	-0.09586542	0.69251754	0.14416344
O	0.12699585	1.40665626	2.48495672
H	-0.33195339	1.02584939	3.25239930
H	1.08619953	1.41253979	2.67733732
O	-0.13403649	3.25299461	0.00251282
H	0.22692486	3.76360738	-0.74174331
H	-0.23595600	3.87430780	0.74288701
O	-1.61126022	0.95997941	-1.96597278
H	-1.93401758	0.03237110	-1.91797476
H	-2.35436471	1.51860589	-2.24711877
O	1.07442312	1.26915759	-1.96108883
H	0.46658572	1.14473799	-2.71437533
H	1.94642425	0.93359305	-2.23060808
O	-2.34900702	0.52727071	1.24100606
H	-2.67715068	-0.32245054	0.88237911
H	-3.09312033	0.99847771	1.64947100
O	-1.20351251	-1.12904616	-0.45180967
O	2.41345367	1.19449576	1.06735004
C	0.85950815	-2.24983507	0.13535064
C	-0.61631778	-2.33587410	-0.39516255
O	-1.13320926	-3.37718862	-0.70915324
O	1.57083727	-3.21233285	0.25615518
O	1.21885851	-0.98424791	0.42333237
H	3.22937102	1.71225884	0.97186021
H	2.64185864	0.24057277	0.99181439

3. $[Lu(ox)(H_2O)_6]^+$

E_{gas} = -2072.069428567514
E_{water} = -2072.243333029937
$E_{ZPE/Th}$ = 0.371937

Lu	0.06250202	0.50545453	-0.29413892
O	0.37133999	1.16593532	2.08873975
H	0.85597277	1.85709190	2.56882667
H	0.75962519	0.29508016	2.33738880
O	-0.06796213	2.91900863	-0.42314241
H	0.18618697	3.36014558	-1.25232991
H	-0.59794780	3.55484015	0.08602389
O	-1.72881128	0.73539835	-2.11343099
H	-1.83730721	-0.24117477	-2.19008555
H	-2.58798119	1.15798138	-2.27572585
O	0.87895858	1.14369363	-2.45117541
H	0.16379396	1.00676708	-3.10213290
H	1.69148504	0.75901797	-2.82254338
O	-1.96655888	0.60597796	0.90459859
H	-2.68295262	-0.03508874	0.75497265
H	-1.84523708	0.68729727	1.86838236
O	-0.61164192	-1.30769294	-1.14627665
O	2.46396054	0.65782843	-0.23244007
C	0.60589108	-2.34889500	0.66002677
C	-0.32218792	-2.49783636	-0.59900850
O	-0.72288759	-3.56304151	-0.99293161
O	1.00344454	-3.29016429	1.29722336
O	0.88657762	-1.06059236	0.92224823
H	3.20032069	1.29053676	-0.25025994
H	2.71266167	-0.10053500	0.33462446

4. $[La(NO_3)_3(H_2O)_2]$

E_{gas} = -1429.734574971542
E_{water} = -1429.793426397650
$E_{ZPE/Th}$ = 0.210857

La	-0.12468647	1.03223516	0.12151561
O	-0.93905598	1.62999390	2.43424068
O	-0.93998851	3.25867643	0.98605196
N	-1.18781716	2.87489732	2.19452617
O	-1.62080881	3.62578086	3.03927581
O	0.34891303	2.01745249	-2.16408180
O	2.08180317	1.34733666	-1.03174303
N	1.62940873	1.88293465	-2.12341318
O	2.35723326	2.22500380	-3.02517221
O	-1.32908675	-1.01871618	-0.67906730
O	0.22758559	-1.38421850	0.79651749
N	-0.68497633	-1.88658612	0.03869064
O	-0.92722959	-3.06946951	-0.00613520
O	-2.52138440	1.44869500	-0.77150003
H	-3.00196893	0.74717127	-1.24298326
H	-2.94480589	2.29816784	-0.97541607
O	1.91905635	1.22754967	1.70267643
H	1.95866306	1.04367462	2.65508877
H	2.82360488	1.19455791	1.34758470

5. $[Gd(NO_3)_3(H_2O)_2]$

E_{gas} = -1759.794226672427
E_{water} = -1759.848820757216
$E_{ZPE/Th}$ = 0.207574

Gd	-0.13513919	1.05072306	0.14172245
O	-0.99217529	1.54680671	2.33329686
O	-0.81353890	3.21374674	0.94486515
N	-1.15280584	2.81298793	2.12641199
O	-1.58586068	3.56255484	2.97065460
O	0.22143881	2.06945902	-2.01217962
O	1.93252895	1.14074484	-1.04861900
N	1.47625640	1.78234850	-2.08144397
O	2.17270588	2.07944558	-3.02084387
O	-1.11879082	-0.91884335	-0.78196202
O	0.22463974	-1.20740215	0.90050822
N	-0.54739040	-1.75840592	0.02751234
O	-0.72794476	-2.94952554	-0.03891621
O	-2.43360278	1.47152434	-0.63936449
H	-2.84495669	0.82565298	-1.23860507
H	-2.73517697	2.35843811	-0.89662105
O	1.77786415	1.29878124	1.67441624
H	1.73654499	1.00547351	2.59962957
H	2.66986265	1.11062683	1.33619405

6. $[Lu(NO_3)_3(H_2O)_2]$

E_{gas} = -2230.383316640299
E_{water} = -2230.4438958790816
$E_{ZPE/Th}$ = 0.213662

Lu	-0.10477591	1.05749453	0.25050460
O	-1.19973466	1.80224343	2.14235382
O	-0.24762511	3.29170219	0.88547897
N	-0.93743681	3.05785430	1.94968877
O	-1.30886955	3.92642920	2.70303319
O	0.02996923	1.85914963	-1.91210950
O	1.86853724	1.66578223	-0.78563868
N	1.31459621	2.00682299	-1.90324244
O	1.93720397	2.42322588	-2.84793501
O	-0.85894362	-0.92430874	1.16531048
O	0.24459836	-1.03848144	-0.69853465
N	-0.37767299	-1.68253618	0.22938148
O	-0.50386569	-2.88420111	0.23192706
O	-2.25749349	1.13280015	-0.64374294
H	-2.43237406	1.44135590	-1.54896173
H	-3.09999949	0.90675244	-0.21834996
O	1.65037162	0.71558329	1.74791157
H	1.61870613	0.35400736	2.64798844
H	2.57487175	0.90677754	1.51561660

5. Thermal Characterization

Differential scanning calorimetry (DSC) was performed with a computer-controlled Phoenix DSC 204 F1 thermal analyzer (Netzsch, Germany) with nitrogen as the protection gas. The samples were placed in aluminum pans. Experimental data is displayed in such a way that exothermic peaks occur at negative heat flow and endothermic peaks at positive heat flow. DSC runs included heating and subsequent cooling at 10°C/min. Given temperatures correspond to the onset of the respective thermal process. Thermogravimetric analyses were carried out in a dry air stream on a STA 449 F3 Jupiter (Netzsch, Germany) in sealed (pierced) aluminum pans.

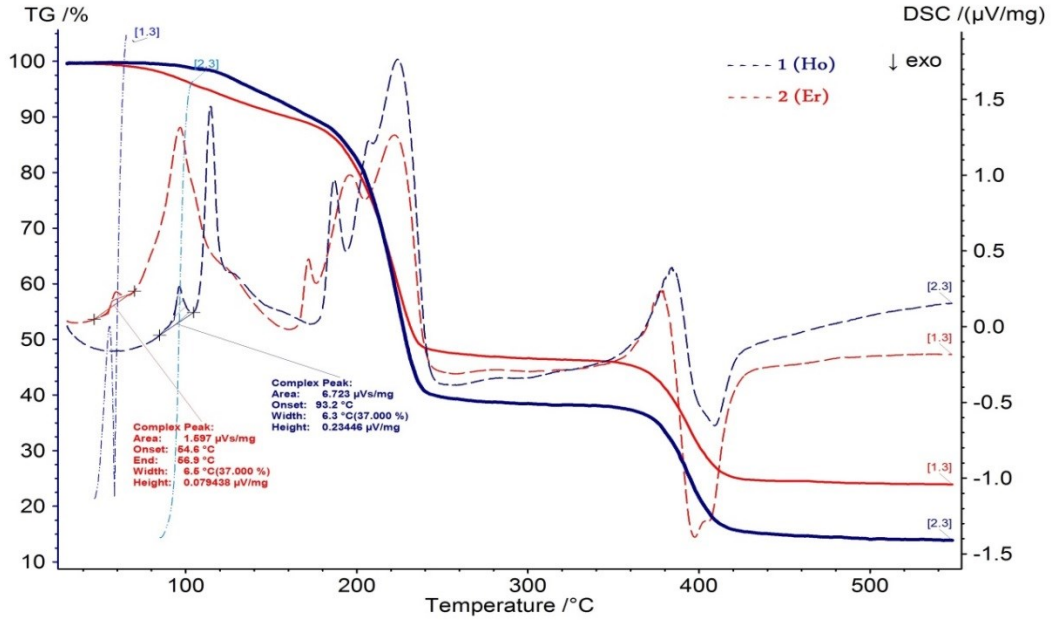

Figure S8. TG (solid line)/DTA(dotted line) traces of the crystalline **1** and **2** compounds at a heating rate of 10 °C·min^{-1} under a nitrogen atmosphere.

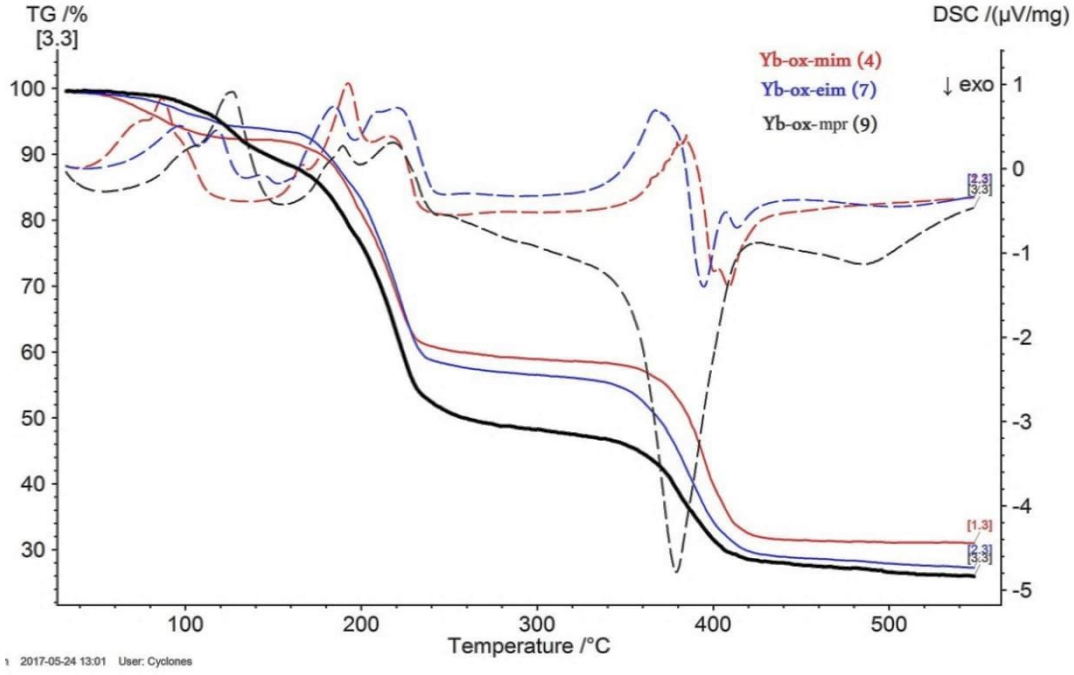

Figure S9. Thermal decomposition of ytterbium containing oxalates (**4**, **7** and **9**) under streaming nitrogen (20 mL/min) on heating at 10 °C/min – TG (solid line), DTA (dotted line).